

Properties and structure of SPEEK proton exchange membrane doped with nanometer CeO₂ and treated with high magnetic field

J. Y. Tong^{1,2}, Q. Guo^{1*}, X. X. Wang¹

¹School of Materials Science and Engineering, Shanghai University, Shanghai, 201800, China

²School of Wenling, Zhejiang TV University, Wenling, 317500, China

Received 18 July 2009; accepted in revised form 1 October 2009

Abstract. The membranes of sulfonated polyetheretherketone (SPEEK) doped with rare earth metal oxide nanometer cerium oxide (CeO₂) were prepared for direct methanol fuel cell (DMFC) application, which was treated by parallel or perpendicular high magnetic field of 6 Teslas (T) at 100°C. The proton conductivity of membrane specimens increased with temperature raised from 20 to 60°C and decreased with increasing CeO₂ contents. The proton conductivity of membrane specimens under treatment with high magnetic field was better than that without treatment. The membrane specimens treated with perpendicular magnetic field demonstrated better proton conductivity than those treated with parallel magnetic field. The methanol permeation coefficient of membrane specimens decreased with increasing CeO₂ contents and furthermore reduced by about 20% after treated with perpendicular high magnetic field. The water uptake of membrane specimens decreased with CeO₂ doping, but would not be influenced by the magnetic field. Fourier transform infrared spectroscopy (FTIR) and small-angle X-ray scattering (SAXS) revealed certain reaction between oxygen anion in sulfonic groups and cerium cation in the CeO₂ which dispersed evenly in the membranes but formed small conglomerates as shown by the atomic force microscopy (AFM) images. X-ray diffraction (XRD) proved the stability of the crystal structure of the nanometer CeO₂ in polymer membranes, indicating that the reaction occurred only at the interface between SPEEK resin and CeO₂ particles.

Keywords: polymer membranes, SPEEK/CeO₂, high magnetic field, methanol permeability

1. Introduction

Sulfonated polyetheretherketone (SPEEK) has attracted considerable attention as proton exchange membrane (PEMs) for direct methanol fuel cell (DMFC) applications, since it possesses good thermal stability and mechanical property [1–4]. However, increasing degrees of sulfonation (DS) of SPEEK materials have a negative effect on the proton conductivity and methanol permeability of DMFC. The PEMs with high DS have good proton conductivity, and meanwhile they have high methanol permeability [4–6]. Therefore, the com-

prehensive excellent properties of PEMs can not be obtained at the same time by adjusting DS. Nunes *et al.* [7] claimed a remarkable reduction of the methanol permeability with SiO₂, TiO₂ or ZrO₂ modification in SPEEK. Siliva *et al.* [8] pronounced a reduction of the methanol permeability and proton conductivity via the modification with ZrO₂. Chang *et al.* [9] also published a decreasing methanol cross-over by embedding laponite and montmorillonite into SPEEK matrix. However, the proton conductivities of composite membranes decreased somewhat. Good results have been

*Corresponding author, e-mail: guoq@shu.edu.cn
© BME-PT

obtained by introducing CeO₂ catalyst in proton exchange membrane fuel cell (PEMFC), the performance of the cathode in cell was also improved [10] and CO was removed from H₂ stream without oxidizing excess H₂ on the anode [11]. Nobody has reported the PEMs based on SPEEK doped with nanometer CeO₂ so far.

The high magnetic field can transfer the energy to the material at the atomic-scale without contact and does not change its components. Brijmohan and Shaw [12] has reported that SPEEK-based membranes doped with γ -Fe₂O₃ exhibited better properties for application in PEMs after 0.1 Tesla (T) magnetic field treatment. To our knowledge, however, the use of high magnetic field has not been reported for PEMs in DMFC before. In this paper, polymer membranes were prepared by introducing nanometer CeO₂ in SPEEK, and then treated by high magnetic field parallel or perpendicular to the surface of the membrane, applied for one hour at 100°C. The properties and structure of the polymer membranes were investigated as well as their relative mechanisms.

2. Experimental

2.1. Membrane preparation and high magnetic field treatments

Poly(etheretherketone) (PEEK) was obtained from Jilin University(Jilin, China), in the form of particle. It was dried in a vacuum oven at 100°C overnight. Thereafter, 20 g of polymers were dissolved in 1 l concentrated sulfuric acid (95–98%) (Sinopharm Chemical Reagent Co., Ltd, Shanghai, China) and vigorously stirred at room temperature for 68 hours. Then, the polymer solution was gradually precipitated into ice-cold water under mechanical agitation. The polymer suspension was left to settle overnight. The polymer precipitate was filtered, washed several times with deionized water until pH 7 was achieved and dried at 60°C for 24 h, further dried at 100°C for 2 h. The DS of SPEEK,

48.3%, was determined by titration [9]. After SPEEK was triturated, it was dissolved in dimethylacetamide (DMAc) offered by Sinopharm Chemical Reagent Co., Ltd(Shanghai, China), to make a 10 wt% solution. The mixture was doped with a certain amount of CeO₂ with a particle size of 40–50 nm, offered by Shanghai Huaming Gaona Rare Earth New Materials Co., Ltd (Shanghai, China), and stirred at room temperature for 4 h, afterward at 75°C for 6 h. The pure SPEEK and SPEEK/CeO₂ polymer membranes were obtained by casting their viscous solution onto a glass plate. The glass plate was then dried at 60°C for 48 h to remove the solvents, annealed at 120°C for 4 h. The thickness of the dried membranes was about 100 μ m.

The membranes were placed in a sample cabin of 6T superconducting magnet, Oxford Instruments (Oxford, UK), at 100°C for 1 h. The magnetic induction lines were perpendicular or parallel to the membrane surface in Figure 1a or 1b, and described with letter *E* or *A* in designation of membrane specimens in Table 1, respectively.

Table 1 shows the designation of membrane specimens, where UNT refers to membranes untreated with high magnetic field and MT denotes high magnetic field treatment. MTA and MTE represent the membranes treated with parallel and perpendicular magnetic field, respectively. The number denotes the mass percent of doped CeO₂ particles.

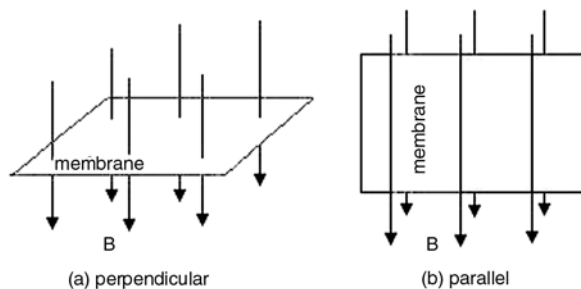


Figure 1. Diagram of magnetic vector with surface of membrane specimen (a) perpendicular or (b) parallel

Table 1. Designation of membrane specimens

CeO ₂ content [wt%]	Untreated with magnetic field (UNT)	Magnetic field treatment(MT)	
		Perpendicular (E)	Parallel (A)
0	UNT-0	MTE-0	MTA-0
2	UNT-2	MTE-2	MTA-2
5	UNT-5	MTE-5	MTA-5
8	UNT-8	MTE-8	MTA-8

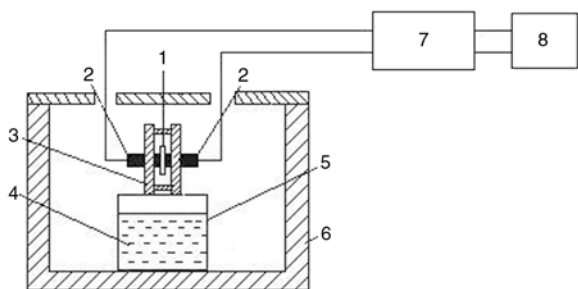


Figure 2. Schematic diagram of conductivity measurement device. 1 – membrane, 2 – electrode, 3 – insulator clamp, 4 – water, 5 – beaker, 6 – adiabatic groove, 7 – Solartron Instruments, 8 – computer

2.2. Proton conductivity measurements

The proton conductivity of membrane specimens in the traverse direction was measured in a measurement cell using AC electrochemical impedance spectroscopy (EIS), which was composed of a Solartron Instruments 1287 electrochemical interface and a Solartron Instruments 1255B frequency response analyzer (Farnborough, UK), both of which were interfaced via GPIB to a computer as shown in Figure 2. The EIS was recorded over a frequency range of 1–10⁶ Hz, the amplitude of the sinusoidal modulation voltage was 10 mV, and the temperature ranged from 20 to 60°C. The membrane specimen in a beaker which contains temperature controller was clamped between two gold-plated copper electrodes (home-made, diameter 4.30 mm) with a constant pressure and relative humidity of about 75%. Before the test, all membrane specimens were soaked in deionized water for 24 h. The proton conductivity σ was calculated by Equation (1):

$$\sigma = \frac{l}{AR} \quad (1)$$

where σ [S·cm⁻¹] was the proton conductivity, l [cm] and A [cm²] were the thickness and area of the membrane specimen, respectively, and R [Ω] was derived from the high frequency intercepting with the real axis on a complex impedance plane plot.

2.3. Methanol permeability and water uptake

A group of different concentrations of methanol solution were prepared. 4.04 ml methanol (density 0.792 g·ml⁻¹) from Sinopharm Chemical Reagent

Co., LtdS (Shanghai, China) and 95.96 ml deionized water were placed in 100 ml measuring flask to make a methanol solution with molar concentration of 1.00 mol·l⁻¹, and then the solution was kept in cryopreservation as a standard solution. Twelve different volumes varying from 25.0 μ l to 0.600 ml, with an average increase of 25.0 μ l, were drawn from the standard solution, and then placed in 25 ml measuring flask to obtain specific methanol solution with concentration from 1.00·10⁻³ to 1.20·10⁻² mol·l⁻¹. The retention time and peak area were recorded after injecting 10.0 μ l solution taken from the twelve samples in GC9800 gas chromatograph, Shanghai Kechuang GC Instrument Co., Ltd (Shanghai, China), immediately at room temperature, and each experiment was performed five times. The maximum relative error calculated from the average was less than 3.46%, demonstrating the peak area vs. methanol concentration curve could be applied to the quantitative analysis. The standard curve of the different concentration of methanol and the peak area is shown in Figure 3.

The methanol permeability coefficient was determined by a home-made diaphragm diffusion cell, which was identical to that described in [2], consisting of two half-cells separated by a membrane. 70 ml 5 M methanol solution was placed on one side of the diffusion cell and deionized water of the same volume was placed on the other side. Magnetic stirrers were used in both compartments to ensure uniformity. The peak areas were converted into methanol concentration in the compartment of deionized water with a reference to above-mentioned calibration curve in Figure 3. The methanol permeability coefficient P [cm²·s⁻¹] was calculated

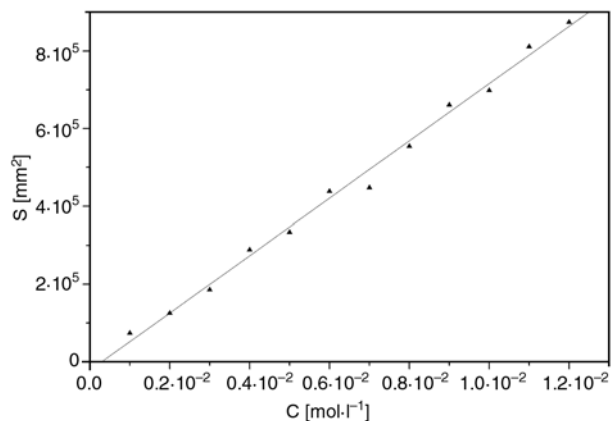


Figure 3. The curve of peak area versus methanol concentration

from the Equation (2) derived from the second law of Fick's diffusion:

$$P = \frac{sV_2l}{AC_{10}} \quad (2)$$

where s [$\text{mol}\cdot\text{l}^{-1}\cdot\text{s}^{-1}$] was the slope of the straight-line plot of the methanol concentration versus permeation time, V_2 [ml] was the volume of deionized water, l [cm] and A [cm^2] were the thickness and area of membrane, respectively, C_{10} [$\text{mol}\cdot\text{l}^{-1}$] was the initial concentration of methanol solution. All membrane specimens were immersed in deionized water for 24 h before testing, and then the thickness and area of wet membranes were measured. Thereafter, the membrane specimens were stabilized at test temperature for more than 1 h, and then placed in diffusion cell for the measurement of methanol permeability.

The water uptake (S_w) of the membrane specimens was calculated by measuring the weight difference between the dry and hydrous membrane specimens [13]. The dried membrane specimens at 90°C for 24 h were weighed ($mass_{dry}$) and then immersed in deionized water for 24 h. Then the membranes were wiped with blotting paper to remove the surface water and quickly weighed ($mass_{wet}$) again. The S_w was calculated with Equation (3):

$$S_w = \frac{mass_{wet} - mass_{dry}}{mass_{dry}} \cdot 100\% \quad (3)$$

2.4. Structure of morphology

The surface and cross-section morphology of the membrane specimens were investigated by a scanning electron microscope HITACHI S-4800 (SEM) (Tokyo, Japan). The surface morphology was also studied by a scanning probe atomic force microscopy ZL AFM-III (AFM), Shanghai Zhuolun MicroMano Co., Ltd (Shanghai, China) in tapping mode. The surface of the membrane specimens was not pretreated while the cross-section of the membrane specimens was pretreated by freezing dry membrane in liquid nitrogen. The fresh cryogenic fracture of the membrane specimens was sputtered with a thin layer of Au in vacuum prior to SEM measurements.

Fourier Transform Infrared (FTIR) spectra of the dry membrane specimens were collected using a Nicolet-AVATAR380 FTIR, Thermo Nicolet Cor-

poration (Madison, USA), spectrometer in frequency range of $300\text{--}2000\text{ cm}^{-1}$. The specimens were prepared by making KBr pellets composed of polymer membrane.

X-ray diffraction (XRD) of the membrane specimens was carried out with a Rigaku D\max2550 (Akishima, Japan), using a Cu-Pd radiation and operated at 40 kV and 200 mA. The XRD patterns were collected with a scan rate of $7^\circ\cdot\text{min}^{-1}$ in the range of from 10 to 70° . The small angle X-ray scattering (SAXS) experiments of membrane specimens were performed at a SAXS MAX 3000 (Rigaku) with $\text{CuK}\alpha$ radiation, collected with a scan rate of $0.09^\circ\cdot\text{min}^{-1}$ at room temperature. The explored q was the range of $0\text{--}0.20\text{ \AA}^{-1}$ for SAXS measurement, where q was the modulus of the scattering vector.

3. Results

3.1. Proton conductivity of membranes

Figures 4–7 are the curves of proton conductivity of pure SPEEK and polymer membranes with 2, 5, 8 wt% CeO_2 contents at $20\text{--}60^\circ\text{C}$ and about 75% relative humidity, respectively. The conductivity of all membrane specimens increased with temperature and was higher than $10^{-2}\text{ S}\cdot\text{cm}^{-1}$, which is the lowest value for practical interest in fuel cell [13] when the temperature exceeded 40°C in Figure 4. The proton conductivity of specimens treated by high magnetic field increased obviously, and the MTE membrane specimens demonstrated better conductivity than the MTA ones. Compared with pure SPEEK membrane in Figure 4, the conductivity of polymer membranes decreased in Figure 5, which may be due to the introduction of CeO_2 into

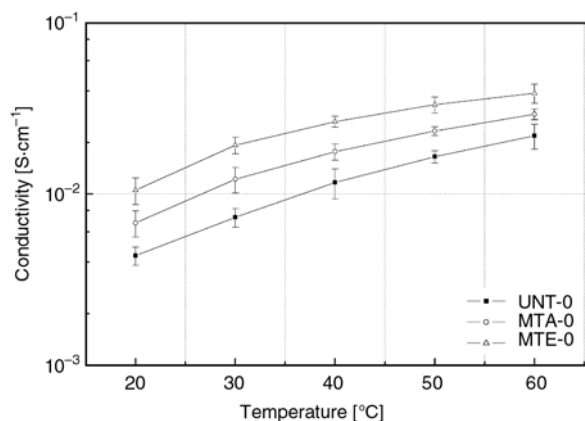


Figure 4. Conductivity of pure SPEEK membrane specimens as a function of temperature

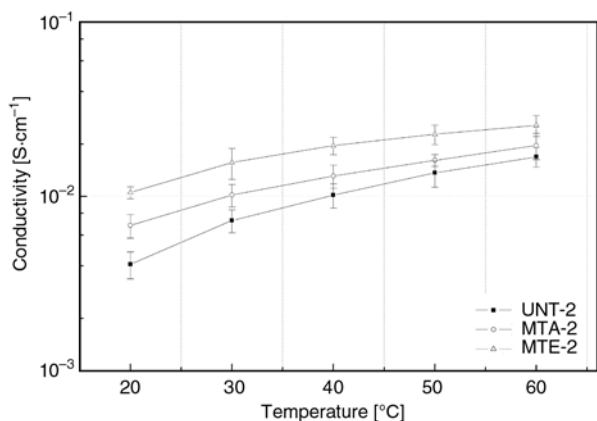


Figure 5. Conductivity of 2 wt.% CeO₂ membrane specimens as a function of temperature

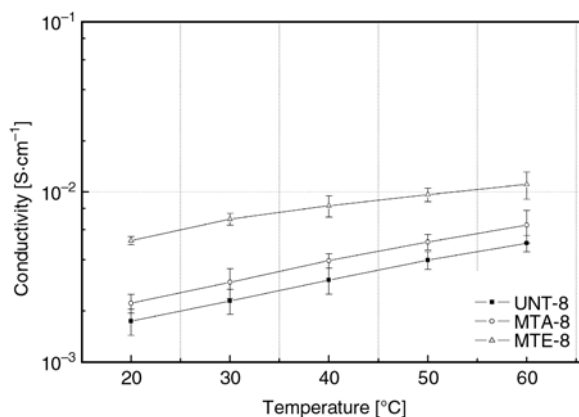


Figure 7. Conductivity of 8 wt.% CeO₂ membrane specimens as a function of temperature

the SPEEK matrix, resulting in reaction between the CeO₂ and the sulfonic groups in SPEEK. However, the conductivities of MTA-2 and MTE-2 were higher than that of the UNT-0 below 50°C. A probable reason was that the polar groups with treatment of high magnetic field played a role in enhancing the proton conduction. As shown in Figure 6, the conductivities of polymer membranes increased with temperature and showed the same tendency in Figure 4 or 5 though with slight improvement. The conductivities of the MTE-5 and MTA-5 within the test temperature both reached 10⁻² S·cm⁻¹. The proton conductivity of MTA-8 was somewhat higher than that of UNT-8 but both of them failed to reach 10⁻² S·cm⁻¹ in Figure 7. The conductivity of MTE-8 was improved dramatically, approaching 10⁻² S·cm⁻¹ at 50°C and exceeding 10⁻² S·cm⁻¹ at 60°C.

The test temperature was controlled up to 60°C because the relative error of the conductivities increased with temperature as a whole, particularly above 60°C. As shown in Figures 4–7, the conduc-

tivities of all membrane specimens improved with temperature, in particularly UNT-0, reaching 1.688·10⁻² S·cm⁻¹ at 60°C, which was five times higher than at 20°C. With CeO₂ doped in SPEEK matrix, the conductivities of polymer membranes decreased gradually. However, it was apparent that the conductivities of all membrane specimens remarkably increased after treatment of high magnetic field and were higher than 10⁻² S·cm⁻¹ except MTA-8, which proved reorientation or deformation of the polar groups in membrane induced by magnetic field, facilitating the proton conduction. At the same time, it was found that the sensitivity of conductivity versus temperature was weakened with increasing CeO₂ contents.

3.2. Methanol permeability and water uptake

Figure 8 plots the fitted lines of methanol concentrations for various specimens against time in the compartment of the deionized water by gas chromatography based on the calibration curve shown

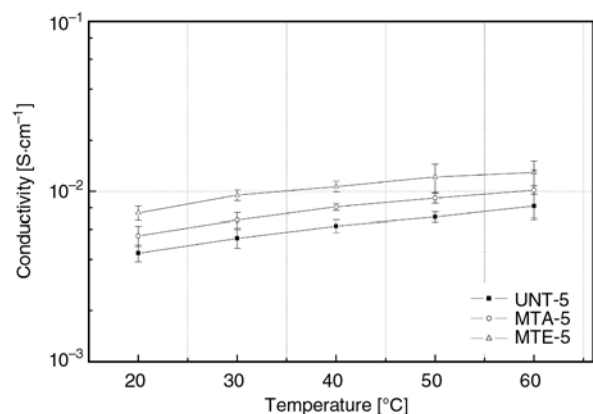


Figure 6. Conductivity of 5 wt.% CeO₂ membrane specimens as a function of temperature

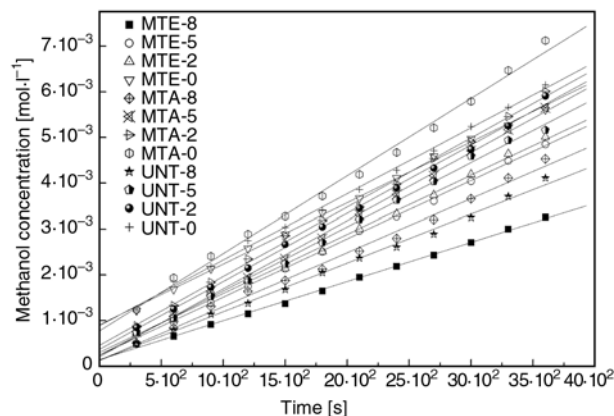


Figure 8. The relationship of methanol diffusion versus time at room temperature

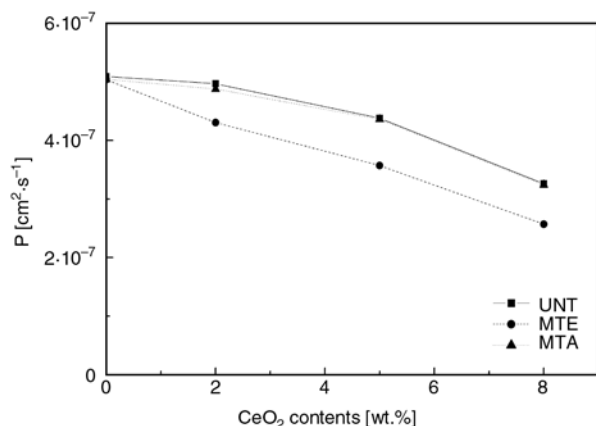


Figure 9. The curve of methanol permeation vs. contents of CeO₂

in Figure 3. The methanol permeability coefficient P was calculated by Equation (2).

Figure 9 shows the relationship of methanol permeability coefficient P versus the nanometer CeO₂ contents at room temperature. The coefficient of UNT-0 reached $5.092 \cdot 10^{-7} \text{ cm}^2 \cdot \text{s}^{-1}$, which was the highest in all tested specimens but an order of magnitude lower than that of the current commercial fluoride membrane. The methanol permeation resistance has not been influenced by magnetic field in the pure SPEEK membrane, but would increase with more CeO₂ doped in polymer membranes, which showed a tendency contrary to the proton conductivity. A possible reason of this is might be that CeO₂ reacts with sulfonic groups, decreasing obviously the methanol permeability as well as weakening somewhat the proton conductivity in the polymer membrane. The methanol permeation resistance of polymer membranes has not been influenced by parallel treatment with high magnetic field but was significantly influenced by perpendicular treatment. The main possible reason was that the polar groups were re-orientated or deformed by the magnetic field in parallel treatment, forming the polar network with a random distribution and enhancing the ordering characteristics, promoting the proton conductivity in some extent, but lowering the methanol resistance. After polymer membrane was treated with perpendicular magnetic field, the polar groups also went through the reorientation or deformation, resulting in similarly layered network with improved ordering characteristics. The ordered array of polar groups contributed to the proton conduction and the layered network structure further hindered the methanol

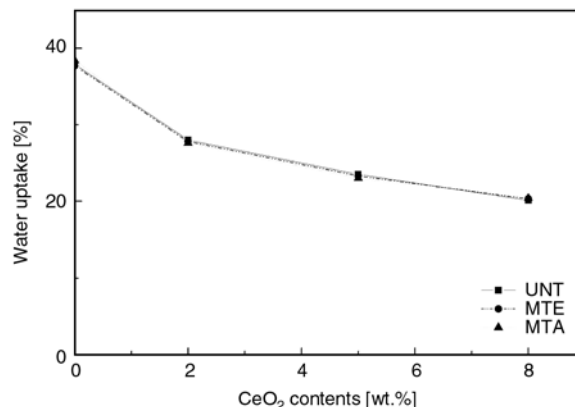


Figure 10. The curve of water uptake vs. CeO₂ content

diffusion in membrane, not only facilitated the proton conduction but also improved the performance of methanol resistance in membrane.

The water uptake of membranes changed with different CeO₂ contents, as shown in Figure 10. The water uptake of the polymer membranes as well as their proton conductivity in Figures 4–7 decreased with CeO₂ contents, opposite to their methanol permeability in Figure 9. This was because the amount of hydrophilic sulfonic groups decreased after being doped with alkaline CeO₂, resulting in smaller hydrophilic regions, or the proton conduction became restricted by the reaction between the CeO₂ and the sulfonic groups, leading to less protons involved in conduction. The water uptake has not been influenced by high magnetic field, which demonstrated the magnetic force only induced the reorientation or deformation but didn't change the amount of the polar groups in accordance with the theoretical expectations.

3.3. Structure of membrane

Figure 11 shows the AFM morphology of two dry membrane specimens, (a) MTA-2 and (b) UNT-5. The membrane surface has a nonporous structure, without cracks, groove marks or phase separation, indicating that it was smooth and compact. The nanometer CeO₂ was dispersed evenly but aggregation still could be observed, about 300 nm in size. With increasing CeO₂ contents, the membrane was denser with lower methanol permeability (as shown in Figure 9), decreased proton conductivity (Figures 4–7) and water uptake (Figure 10).

The typical specimens of UNT-0 and UNT-5 were chosen for the unobserved difference of the MT or

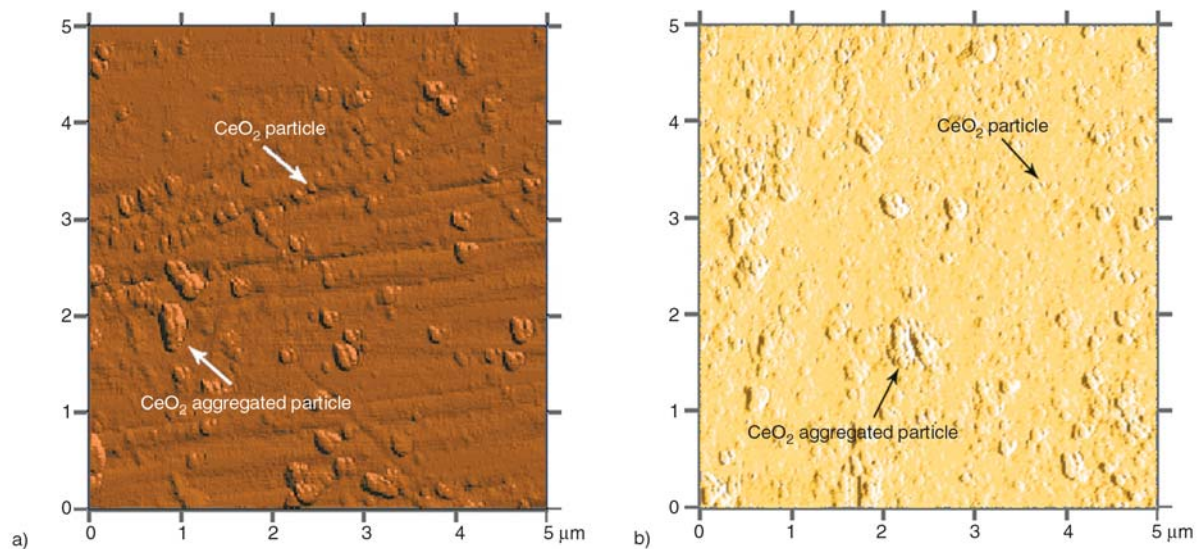


Figure 11. AFM of the MTA-2 (a) and UNT-5 (b) membrane specimens

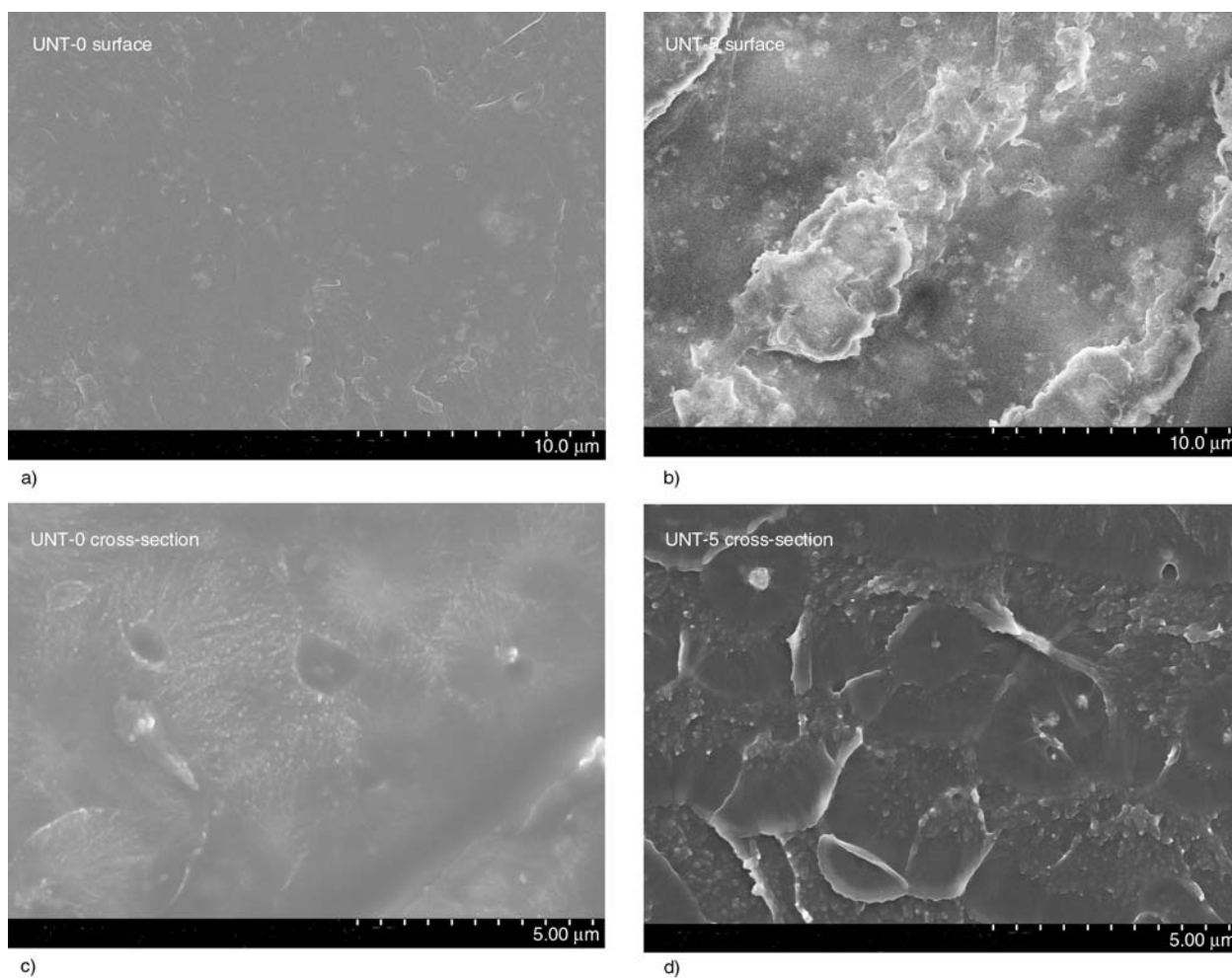


Figure 12. SEM of UNT-0 and UNT-5 membrane specimens surface (a, b) and cross-section (c, d)

UNT specimens. Figures 12a and 12b show the surface morphology of UNT-0 and UNT-5 membrane specimens. Some slight wales were observed on the surface of specimens. The surface was essentially smooth in UNT-0 but slight protrusions appeared in

UNT-5, which were possibly formed during preparation of membrane. Cracks, flaws or phase separation were not observed in SEM micrographs, similar to the result in Figure 11b, illustrating the compact structure of the specimen.

Figures 12c and 12d show the cross-section of UNT-0 and UNT-5 membrane specimens, which were frozen by liquid nitrogen followed by gold sputtering. White neat border was observed in the fractures with unobvious contrast, illustrating the smooth cross-section and the amorphous structure of membranes. There was no mesh structure or phase separation, indicating that the membrane material was compact. But the holes in the UNT-0 specimen were some blowholes formed during preparation in SPEEK. Neither micro-phase separation nor meshes and pores was observed in UNT-5 specimen, which illustrated that the polymer membrane was more compact, resulting in higher methanol resistance. The agglomeration of nanometer CeO_2 was not observed in UNT-5, indicating its good dispersion in polymer membrane. Figure 13 illustrates FTIR spectra of UNT-0 and UNT-5 dry membrane specimens. Two specific membrane specimens were chosen to compare their structures due to unobserved difference of the MT or UNT specimen in the FTIR spectra. The characteristic peaks at 1659–1638 and 1240 cm^{-1} were attributed to stretching vibration of $-\text{Ar}-\text{C}(=\text{O})-\text{Ar}-$ and $-\text{Ar}-\text{O}-\text{Ar}-$, respectively. The $\text{O}=\text{S}=\text{O}$ band at 1260 and 1080 cm^{-1} were observed, corresponding to asymmetric and symmetric stretching vibration peaks, respectively. The characteristic peaks of CeO_2 appeared at 740 and 413 cm^{-1} , shifted from 700 and 400 cm^{-1} reported in [14], proved the coordination occurred probably between cerium cation in the CeO_2 and oxygen anion in the sulfonic groups, enhancing the compact structure of membranes (Figures 11 and 12), decreasing the proton conductivity (Figures 4–7) and the methanol permeability (Figure 9).

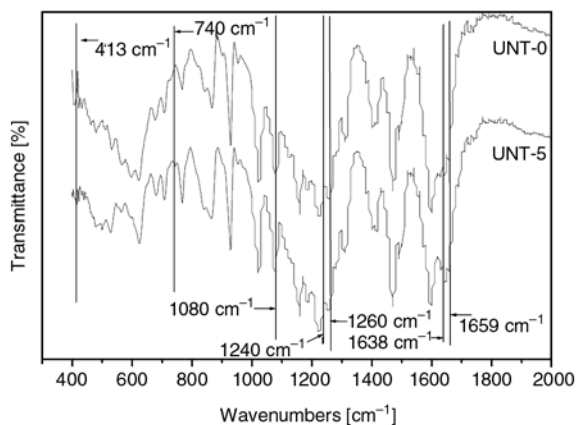


Figure 13. FTIR spectra of UNT-0 and UNT-5 membrane specimens

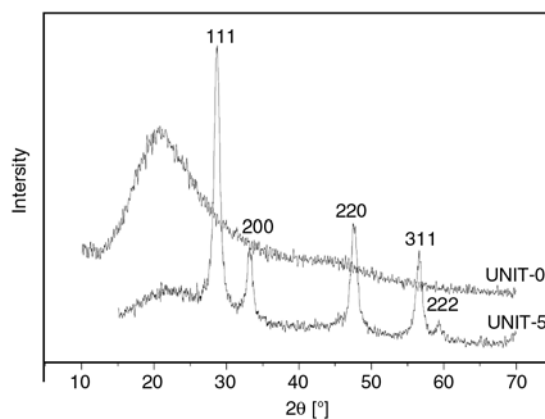


Figure 14. XRD pattern of UNT-0 and UNT-5 membrane specimens

The XRD patterns of UNT-0 and UNT-5 dry membrane specimens are shown in Figure 14. Similarly, the UNT-0 and UNT-5 specimens were chosen to demonstrate that there is no significant effect of the magnetic field on the XRD of the membranes. A typical amorphous diffraction peak could be observed in the UNT-0 specimen [15]. And the diffraction peaks at (111), (200), (220), (311) and (222) in UNT-5 specimen were corresponded with CeO_2 [16], which shows that coordination occurred only at the interface of the two phases.

As shown in Figure 15, there were a uniform broad peak and a shoulder at 0.1679 and 0.1842 Å^{-1} in composite membrane specimens, respectively. A broad peak at 0.1622 Å^{-1} was observed but a shoulder disappeared in UNT-0 specimen. The peak in composite membrane specimens shifted towards larger q -value compared to the plain SPEEK membrane specimen, which demonstrated relatively smaller Bragg spacing ‘center to center distance’ between two clusters or crystallites in composite membrane specimens. A reason for this was that

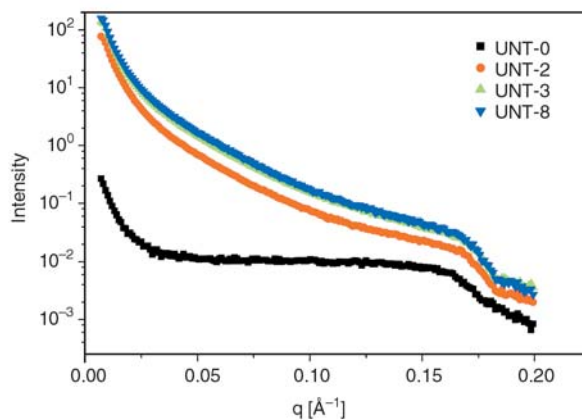


Figure 15. The small-angle X-ray scattering of specimens

sulfonic groups were statistically attached to main chain of SPEEK [17, 18] and the reaction occurred between CeO_2 and sulfonic groups, which increases the compatibility of organic-inorganic materials, thereby decreasing the proton conductivity and enhancing the methanol permeation resistance of specimens.

4. Discussions

There are two mechanisms for proton transport, one via hydrophilic sulfonic groups accompanied by the formation of H_3O^+ or H_5O_2^+ by the reaction of hydration in the hydrophilic regions, and the other is hopping between the adjacent hydrophilic sulfonic groups by H^+ activity. The hydrophilic groups attract water molecules in micro-aqueous phases formed after membrane hydration, increasing the size of hydrophilic regions, shortening the 'effective distance' between sulfonic groups, facilitating the proton transfer in two ways. With increasing temperature, the mobility of proton was enhanced, accelerating transportation between the sulfonic groups gathering in the hydrophilic regions. On the other hand, the water uptake decreased further with temperature, reducing hydrophilic regions in which proton transferred with H_3O^+ or H_5O_2^+ formation. However, the proton conductivity depended on both of them. Therefore, the curve of the conductivity was nonlinear and parabola-shaped, rising with temperature in Figures 4–7. After CeO_2 doping, the AFM of specimens showed that CeO_2 was dispersed evenly in Figure 11. The SEM also demonstrated the compact structure of the membranes with no crack or micro-phase separation observed in the images of Figure 12. The FTIR analysis displayed that the coordination occurred between cerium cation in CeO_2 and oxygen anion in sulfonic groups in Figure 13. The Bragg spacing of organic-inorganic materials was changed as shown in Figure 15, revealing the reaction between CeO_2 and sulfonic groups of SPEEK, decreasing the proton conductivity and methanol permeability, increasing the anti-swelling and mechanical property of polymer membrane, e.g. the methanol permeability of UNT-8 was about 64% and the proton conductivity was 23% of UNT-0 at 60°C, respectively.

It was obvious that the properties of membrane specimens have been influenced by high magnetic field. With appropriate temperature and time, suffi-

cient energy was provided for the polar bonds to rearrange, in particular the ion bonds and the coordination bonds, and the different directions treatment of magnetic field made them to re-orient or deform under the Lorentz forces in certain directions. The high magnetic field with different directions would cause the electron cloud in the polar bonds especially ionic bonds or the coordination bonds to impose different effects on membranes. The change of the electronic cloud shape in polar bonds did not change the chemical structure of the SPEEK and the crystal structure of CeO_2 , however, it had an effect on the proton conductivity and methanol permeability in polymer matrix, but no influence in water uptake for did not change the amount of the sulfonic groups, according to the micro-structural analysis of AFM, SEM, FTIR and XRD, shown above. According to the previous discussion of the reorientation or deformation to the MTE or MTA specimen, the layered network of the polar groups, especially the hydrophilic sulfonic acid groups, was more effective than the random network on properties like proton conductivity or methanol permeability, so the proton conductivity of the MTE was better than that of MTA, and the methanol resistance of the MTE was also effective in improving performance, e.g. the proton conductivity of MTE-8 at 60°C was 1.83 or 2.20 times of MTA-8 or UNT-8 specimen, respectively. The methanol permeability coefficient of the MTE-8 with $2.571 \cdot 10^{-7} \text{ cm}^2 \cdot \text{s}^{-1}$ was about 79% of MTA-8, and also 79% for the UNT-8. The high magnetic field influenced the properties of the proton conductivity and methanol permeability, respectively, but the relevant characterization method has failed to find the mechanism of this impact which has yet to be further explored.

In this paper, the SPEEK with medium DS was chosen. The conductivity of all MTE membrane specimens reached $10^{-2} \text{ S} \cdot \text{cm}^2 \cdot \text{s}^{-1}$, with good methanol resistance and water uptake property, the prepared MTE of polymer membrane specimen as PEMs in DMFC has a certain value.

5. Conclusions

The proton conductivity of the membrane specimen increased with temperature. In addition, the proton conductivity decreased but methanol resistance improved with doping CeO_2 contents in membrane

specimen. It is worth noting that the proton conductivities of all membrane specimens treated with high magnetic field increased obviously, and the MTE membrane specimens demonstrated better conductivity than the MTA. The methanol permeability has been significantly influenced by the treatment with perpendicular high magnetic field. The water uptake of membrane specimens decreased with increasing amount of CeO₂, but remained at the same value after being treated with the magnetic field. The nanometer CeO₂ dispersed evenly in the SPEEK matrix, in which reaction occurred between the cerium cation in CeO₂ and oxygen anion in sulfonic group of SPEEK, enhancing the compatibility of polymer. The polymer membranes treated with perpendicular high magnetic field showed adequate proton conductivity, low methanol permeability, and good stability, having good potential for use in DMFC.

Acknowledgements

The authors gratefully acknowledge Professor Han, C.C. (Institute of Chemistry, Chinese Academy of Sciences, Beijing, China) for the help in SAXS measurements.

References

- [1] Silva V. S., Ruffmann B., Vetter S., Boaventura M., Mendes A. M., Madeira L. M., Nunes S. P.: Mass transport of direct methanol fuel cell species in sulfonated poly(ether ether ketone) membranes. *Electrochimica Acta*, **51**, 3699–3706 (2006). DOI: [10.1016/j.electacta.2005.10.029](https://doi.org/10.1016/j.electacta.2005.10.029)
- [2] Gil M., Ji X. L., Li X. F., Na H., Hampsey J. E., Lu Y. F.: Direct synthesis of sulfonated aromatic poly(ether ether ketone) proton exchange membranes for fuel cell applications. *Journal of Membrane Science*, **234**, 75–81 (2004). DOI: [10.1016/j.memsci.2003.12.021](https://doi.org/10.1016/j.memsci.2003.12.021)
- [3] Rikukawa M., Sanui K.: Proton-conducting polymer electrolyte membranes based on hydrocarbon polymers. *Progress in Polymer Science*, **25**, 1463–1520 (2000). DOI: [10.1016/S0079-6700\(00\)00032-0](https://doi.org/10.1016/S0079-6700(00)00032-0)
- [4] Zaidi S. M. J., Mikhailenko S. D., Robertson G. P., Guiver M. D., Kaliaguine S.: Proton conducting composite membranes from polyether ether ketone and heteropolyacids for fuel cell applications. *Journal of Membrane Science*, **173**, 17–34 (2000). DOI: [10.1016/S0376-7388\(00\)00345-8](https://doi.org/10.1016/S0376-7388(00)00345-8)
- [5] Wilhelm F. G., Pünt I. G. M., van der Vegt N. F. A., Strathmann H., Wessling M.: Cation permeable membranes from blends of sulfonated poly(ether ether ketone) and poly(ether sulfone). *Journal of Membrane Science*, **199**, 167–176 (2002). DOI: [10.1016/S0376-7388\(01\)00695-0](https://doi.org/10.1016/S0376-7388(01)00695-0)
- [6] Xing P. X., Robertson G. P., Guiver M. D., Mikhailenko S. D., Wang K. P., Kaliaguine S.: Synthesis and characterization of sulfonated poly(ether ether ketone) for proton exchange membranes. *Journal of Membrane Science*, **229**, 95–106 (2004). DOI: [10.1016/j.memsci.2003.09.019](https://doi.org/10.1016/j.memsci.2003.09.019)
- [7] Nunes S. P., Ruffmann B., Rikowski E., Vetter S., Richau K.: Inorganic modification of proton conductive polymer membranes for direct methanol fuel cells. *Journal of Membrane Science*, **203**, 215–225 (2002). DOI: [10.1016/S0376-7388\(02\)00009-1](https://doi.org/10.1016/S0376-7388(02)00009-1)
- [8] Silva V. S., Ruffmann B., Silva H., Gallego Y. A., Mendes A., Madeira L. M., Nunes S. P.: Proton electrolyte membrane properties and direct methanol fuel cell performance I. Characterization of hybrid sulfonated poly(ether ether ketone)/zirconium oxide membranes. *Journal of Power Sources*, **140**, 34–40 (2005). DOI: [10.1016/j.jpowsour.2004.08.004](https://doi.org/10.1016/j.jpowsour.2004.08.004)
- [9] Chang J-H., Park J. H., Park G-G., Kim C-S., Park O. O.: Proton-conducting composite membranes derived from sulfonated hydrocarbon and inorganic materials. *Journal of Power Sources*, **124**, 18–25 (2003). DOI: [10.1016/S0378-7753\(03\)00605-0](https://doi.org/10.1016/S0378-7753(03)00605-0)
- [10] Yu H. B., Kim J-H., Lee H-I., Scibioh M. A., Lee J. Y., Han J. H., Yoon S. P., Ha H. Y.: Development of nanophase CeO₂-Pt/C cathode catalyst for direct methanol fuel cell. *Journal of Power Sources*, **140**, 59–65 (2005). DOI: [10.1016/j.jpowsour.2004.08.015](https://doi.org/10.1016/j.jpowsour.2004.08.015)
- [11] Chang L-H., Sasirekha N., Chen Y-W., Wang W-J.: Preferential oxidation of CO in H₂ stream over Au/MnO₂-CeO₂ catalysts. *Industrial and Engineering Chemistry Research*, **45**, 4927–4935 (2006). DOI: [10.1021/ie0514408](https://doi.org/10.1021/ie0514408)
- [12] Brijmohan S. B., Shaw M. T.: Magnetic ion-exchange nanoparticles and their application in proton exchange membranes. *Journal of Membrane Science*, **303**, 64–71 (2007). DOI: [10.1016/j.memsci.2007.06.066](https://doi.org/10.1016/j.memsci.2007.06.066)
- [13] Li X. F., Liu C. P., Xu D., Zhao C. J., Wang Z., Zhang G., Na H., Xing W.: Preparation and properties of sulfonated poly(ether ether ketone)s (SPEEK)/polypyrrole composite membranes for direct methanol fuel cells. *Journal of Power Sources*, **162**, 1–8 (2006). DOI: [10.1016/j.jpowsour.2006.06.030](https://doi.org/10.1016/j.jpowsour.2006.06.030)
- [14] McDevitt N. T., Baun W. L.: Infrared absorption study of metal oxides in the low frequency region (700–240 cm⁻¹). *Spectrochimica Acta*, **20**, 799–808 (1964). DOI: [10.1016/0371-1951\(64\)80079-5](https://doi.org/10.1016/0371-1951(64)80079-5)

- [15] Krishnan P., Park J-S., Kim C-S.: Preparation of proton-conducting sulfonated poly(ether ether ketone)/boron phosphate composite membranes by an in situ sol-gel process. *Journal of Membrane Science*, **279**, 220–229 (2006).
DOI: [10.1016/j.memsci.2005.12.010](https://doi.org/10.1016/j.memsci.2005.12.010)
- [16] Gu H., Soucek M. D.: Preparation and characterization of monodisperse cerium oxide nanoparticles in hydrocarbon solvents. *Chemistry of Materials*, **19**, 1103–1110 (2007).
DOI: [10.1021/cm061332r](https://doi.org/10.1021/cm061332r)
- [17] Prado L. A. S. de A., Wittich H., Schulte K., Goerigk G., Garamus V. M., Willumeit R., Vetter S., Ruffmann B., Nunes S. P.: Anomalous small-angle X-ray scattering characterization of composites based on sulfonated poly(ether ether ketone), zirconium phosphates, and zirconium oxide. *Journal of Polymer Science Part B: Polymer Physics*, **42**, 567–575 (2003).
DOI: [10.1002/polb.10764](https://doi.org/10.1002/polb.10764)
- [18] Prado L. A. S. de A., Goerigk G., Ponce M. L., Garamus V. M., Wittich H., Willumeit R., Schulte K., Nunes S. P.: Characterization of proton-conducting organic-inorganic polymeric materials by ASAXS. *Journal of Polymer Science Part B: Polymer Physics*, **43**, 2981–2992(2005).
DOI: [10.1002/polb.20576](https://doi.org/10.1002/polb.20576)